Research Paper

How the urban morphology impact thermal environment in high-density areas

A city-block-scale study in Harbin, China

Qi AN, School of Architecture and Design, Harbin Institute of Technology; Key Laboratory of National Territory Spatial Planning and Ecological Restoration in Cold Regions, Ministry of Natural Resources, China

Yu DONG, School of Architecture and Design, Harbin Institute of Technology; Key Laboratory of National Territory Spatial Planning and Ecological Restoration in Cold Regions, Ministry of Natural Resources, China

Wei DONG, School of Architecture and Design, Harbin Institute of Technology; Key Laboratory of National Territory Spatial Planning and Ecological Restoration in Cold Regions, Ministry of Natural Resources, China

Abstract

A large number of studies have been conducted to explore the relationship between land surface temperature (LST) and urban morphology. However, few have analysed the diurnal variation of LST and their drivers at the block scale, especially in densely populated urban environments within cold cities. To fill the gaps, this study classified urban blocks into nine types based on building density and height. Using ECOSTRESS LST data, we analysed diurnal differences in LST and assess the influence of block type on LST. Correlation analyses and stepwise regression models were employed to identify key indicators of green space patterns that significantly affect LST intensity. The results indicate that: (1) The spatial distribution of LST varies significantly between day and night. (2) There is a diurnal difference in the effect of urban block classification on LST. During the daytime, building density is the main factor dominating the magnitude of LST intensity. Nighttime, on the other hand, may be related to building height. (3) The results of the correlation analysis and stepwise regression modelling indicate that urban green space patterns is closely related to LST within each type of urban blocks. The results provide new perspectives on urban thermal environment mitigation.

Keywords

Urban heat island, urban block morphology, green space, ECOSTRESS, cold city

1. Introduction

1.1. Urban heat island effects and climate change

As global warming and extreme weather events become more frequent, populations in urban areas will become more sensitive to the combined effects of the urban heat island (UHI) phenomenon and increased heat due to climate change. The urban heat island phenomenon has now been observed in more than 1,100 cities worldwide (Peng et al., 2018). In these cities, the heat island intensity can reach 4 to 5°C and even exceed 10°C in extreme cases (Santamouris, 2020). The UHI effect not only causes negative impacts such as increased energy consumption and deterioration of air quality, but also jeopardizes human health and well-being.The UHI effect is linked to a range of negative outcomes, including elevated energy consumption, deteriorated air quality, and adverse impacts on human health and well-being. Therefore, it is crucial to understand the spatial distribution of urban heat and to analyse its associated influences.

1.2. Thermal management challenges in cold cities

More than 600 million people worldwide live in regions with cold climates. Under the pressure of rapid urbanization, these regions are warming twice as fast as the global average (Welegedara et al., 2023). Therefore, even in colder climates, rapid increases in urban temperatures can expose residents to greater risks. Thermal risk management in cold regions is becoming increasingly urgent. However, a great deal of UHI research is currently focused on warmer cities, with less research on cold areas like Harbin.

1.3. Block-level mitigation of thermal environment in high-density urban areas

Numerous studies have shown that rational urban planning strategies can significantly mitigate UHI. At the same time, remote sensing products such as MODIS, Landsat, and ECOSTRESS provide long time-series and wide-area data coverage, making LST data more easily accessible. However, there are still relatively few studies related to the diurnal variation of LST in densely populated cities. Therefore, we chose the densely populated cold city of Harbin as the study area. Firstly, we obtained the diurnal spatial distribution of LST using ECOSTRESS data. Secondly, blocks were extracted as the basic unit of study, and urban blocks were classified into nine types based on building density and height. We further extracted the landscape characteristics of urban green spaces within each type of block. Subsequently, we calculated distribution indices to assess the effect of block type on LST. Finally, the key factors affecting LST were identified using Pearson correlation analysis and stepwise regression methods, respectively.

2. Methodology

2.1. Study area

Harbin (125°42′–130°10′ E, 44°04′–46°40′ N) is the capital of Heilongjiang Province in Northeast China (Figure 1). The city has a total area of 53,136.94km^2 and 9.395 million residents by the end of 2022. Harbin has a mid-temperate continental monsoon climate, and the temperatures here have consistently increased over the past decade. Our study focuses on the core urban area of Harbin within the fourth ring road. This part of the region covers an area of 4,068.04km^2, has the highest building density, a variety of urban functions and a high population density.

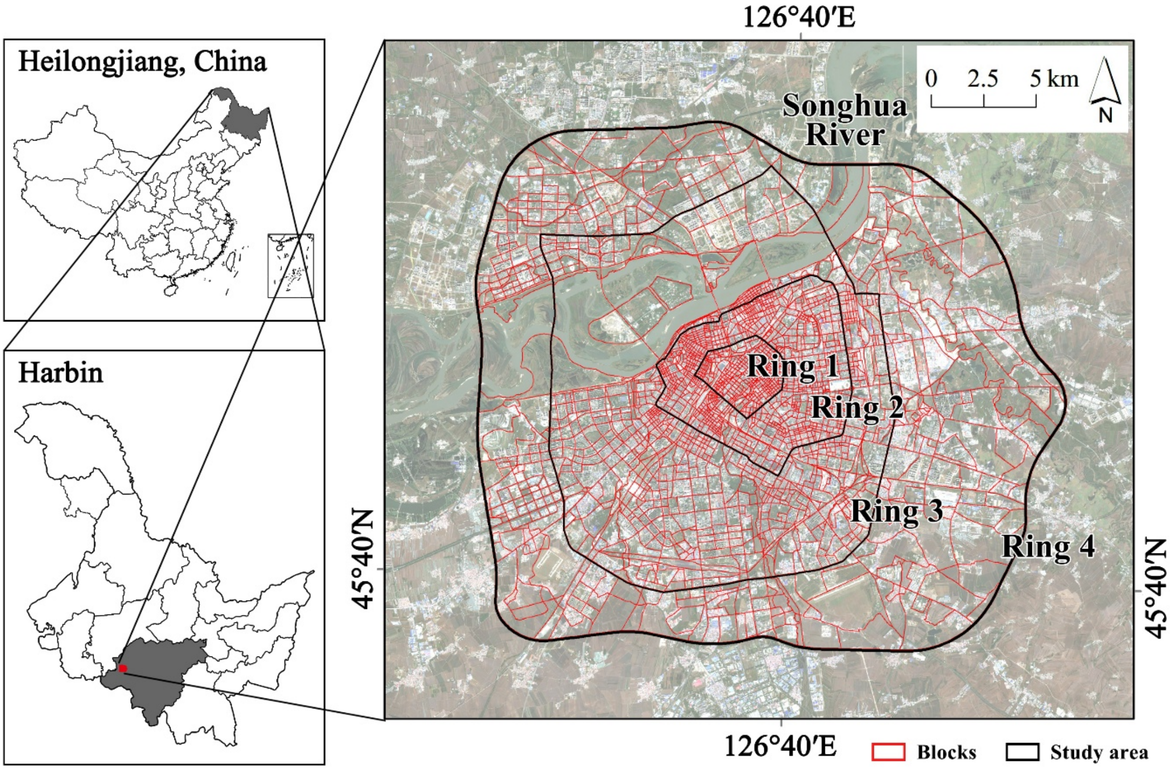

Figure 1. Geographical location map of the study area and blocks. Source: By the authors.

2.2. LST data collection

ECOSTRESS LST products were sourced from the the NASA Land Processes Distributed Active Archive Center (https://lpdaac.usgs.gov/) (Chang et al., 2021). ECOSTRESS instruments operate on the International Space Station orbit. This approach provides diurnal surface temperature at a spatial resolution of 70 meters and a temporal resolution of 3-5 days (Hulley et al., 2019). Previous studies shows strong consistency between ECOSTRESS surface temperature data and other thermal infrared instruments (Hook et al., 2020; Silvestri et al., 2020).

In this study, we used the ECOSTRESS Atmospherically Corrected Surface Temperature and Emissivity Level 2 product (ECO2LSTE) (https://lpdaac.usgs.gov/products/eco2lstev001/). This dataset applies a physically-based Temperature Emissivity Separation (TES) method to derive LST. Our analysis focused on summer, with data from July 2022 to August 2023. We downloaded the ECOSTRESS LST scenes from the AppEEARS tool (https://lpdaac.usgs.gov/tools/appeears/). Two high-quality scenes were aquired at different Beijing time (UTC+8): 10:17 on August 10, 2022, and 19:07 on July 30, 2023 (Table 1). We also verified the LST accuracy using hourly geostationary satellite data from Copernicus Global Land Service (Chang et al., 2021). In ArcGIS, we selected 100 radom sampling points to compare the two datasets. Their Pearson correlation coefficients were 0.843 and 0.773, which indicates a strong linear correlation relationship.

Table 1. Specific information of Landsat imagery and atmospheric correction parameters of LST.

Date acquisition data and time	Maximum value of data /℃	Minimum value of data /℃	Mean value of data /℃	Standard deviation of data	The temperature at the last full hour /℃	Wind speed at the last full	Average daily temperature /℃

						hour /(m·s^{-1})	
2022/08/10 UTC 02:17 UTC+8 10:17	48.8	23.8	33.0	3.9	24.9	3.8	21.9
2023/07/30 UTC 11:07 UTC+8 19:07	27.6	14.0	21.5	1.4	29.3	4	25.3

2.3. Mapping urban blocks

We followed previous studies (Hu et al., 2022; Yao et al., 2023; Zhou et al., 2022) to define block categories. These categories rely on building density (BD) and building height (BH). Stewart and Oke's classification criteria guided this approach (Stewart and Oke, 2012). We divided blocks into three density levels: low (BD＜0.15), medium (0.15≤BD＜0.25), and high (BD≥0.25). We also divided blocks into three hight levels: low-rise (BH＜9m), mid-rise (9m≤BH＜21m), and high-rise (BH≥21 m). These divisions produce nine block categories.

We used building vector data from Baidu map in June 2019 (https://lbsyun.baidu.com/). This dataset includes spatial locations, vertical projection boundaries, and floor counts. Chen et al. (2023) showed that this data can effectively help to study the influence of building form on the SUHI effect. We estimated building height by multiplying the number of floors by three (Sun et al., 2020). And we calculated building density as the ratio of each block's building basal area to its total area. To ensure accuracy, we also used Sentinel-2 imagery from May 10, 2022 to fill any missing data.

2.4. Extraction of urban green space morphological characteristics

In urban areas with dense construction, green spaces offer effective and economical strategies for mitigating thermal environments. We used Fragstats to measure the morphological factors of urban green spaces. These factors include Total Class Area (CA), Percentage of Landscape (PLAND), Patch Density (PD), Landscape Shape Index (LSI), and Aggregation Index (AI) (Table 2). We sourced the urban green space data from the fine-grained urban green space map (UGS-1m) (https://doi.org/10.57760/sciencedb.07049) developed by Shi et al. (2023). This dataset has a spatial resolution of approximately 1.1 m, with an overall accuracy of 87.56% and an F1 score of 74.86%.

Table 2. Description and calculation of urban green space morphological characteristics.

Metrics	Abbreviation	Description	Calculation
Total Class Area	CA	The sum of the area of urban green space in a block	$CA=\sum_{j=1}^{n} a_{ij}\times\frac{1}{10000}$
Percentage of Landscape	PLAND	Proportion of the landscape occupied by urban green space in a block	$PLAND=\frac{\sum_{j=1}^{n} a_{ij}}{A}\times 100$

Patch Density	PD	Patch density of urban green space in a block	$PD = \frac{n_i}{A} \times 10000 \times 100$
Landscape Shape Index	LSI	Irregular degree of urban green space shape in a block	$LSI = \frac{0.25\sum_{k=1}^{m} e_{ik}^{*}}{\sqrt{A}}$
Aggregation Index	AI	Aggregation degree of urban green space shape in a block	$AI = \left[\frac{g_{ii}}{\max \to g_{ii}}\right] \times 100$

Notes：The relevant calculation method comes from https://www.fragstats.org/.

2.5. Influence of urban block categories on LST

In this study, we used the distribution index (DI) to measure the impact of different urban block categories (Yao et al., 2022). The formula is shown as follows:

$$DI = \frac{S_{hi}}{S_i} \Big/ \frac{S_h}{S}$$

We defined high temperature center (HTC) using the temperature threshold method (Zhao et al., 2024). Where S_{hi} and S_i represent the areas of HTC in the i^{th} urban blocks and the entire study area respectively. S_h and S indicate the total area of HTC and the total area of all urban block categories. If the DI of a certain urban block is greater than 1, then the HTC in that block is its main distribution region (Huang and Wang, 2019).

2.6. Main driving factors affecting the LST in urban blocks

We used a Pearson correlation analysis to analyze the relationship between LST and five green space morphological indicators. After that, the factors that are significantly correlated with LST are identified as relevant influences (Yao et al., 2023). Finally, LST and all relevant influences were entered into the stepwise regression model. The main drivers were identified based on the results of the model. The above statistical analysis were completed using SPSS (v20).

3. Results

3.1. Diurnal distribution characteristics of LST

The spatial distribution of LST at different observation times is shown in Figure 2. Fig. 2a shows the LST during the day (10:17 local time). Fig. 2b shows the LST at night (19:07 local time). The daytime LST in the study area is 23.77°C to 48.75°C, with an average of 33.02°C. The LST at night is 14.05°C to 27.61°C, with an average of 21.51°C. These values show that the distribution of LST has obvious diurnal differences. Figure 3 shows the spatial distribution of urban green space and related land use. The study area is densely populated, with important infrastructure such as Harbin Railway Station and large shopping mail. Nearby industrial facilities, including Harbin Boiler Factory and Harbin Pharmaceutical Group, may also cause the increase of LST. The LST of water body and forest is low during the day. This discovery also supports the previous research results that blue-green space is conducive to cooling down. At night, the LST of Songhua River and nearby middle and high-rise buildings is higher. This may be due to the high specific heat capacity of water body and the slow release of heat. High-rise buildings will also retain heat until night. Therefore, even if there is no direct sunlight at night, these areas will maintain a high LST.

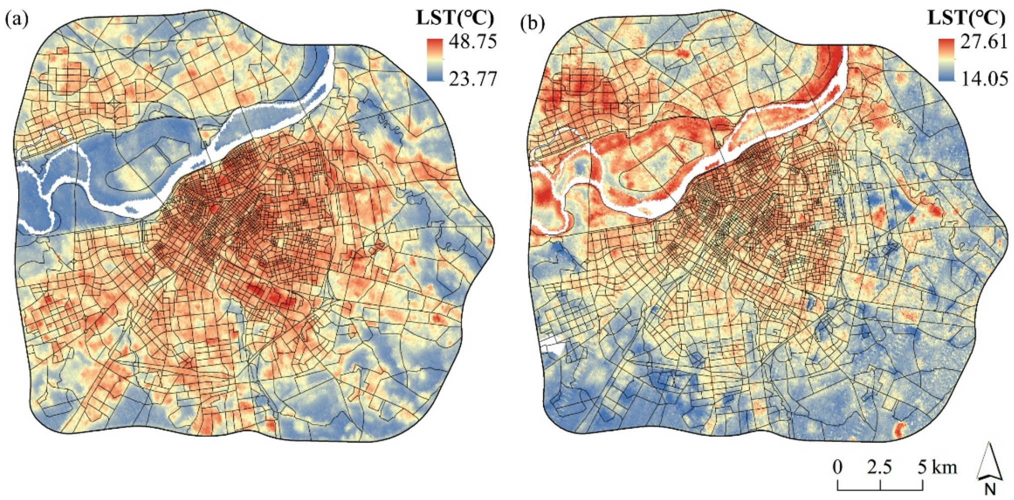

Figure 2. Spatial distribution of LST at different observation times. (a) 10:17; (b) 19:07. The white area in the map has been removed because it was covered by clouds. Source: By the authors.

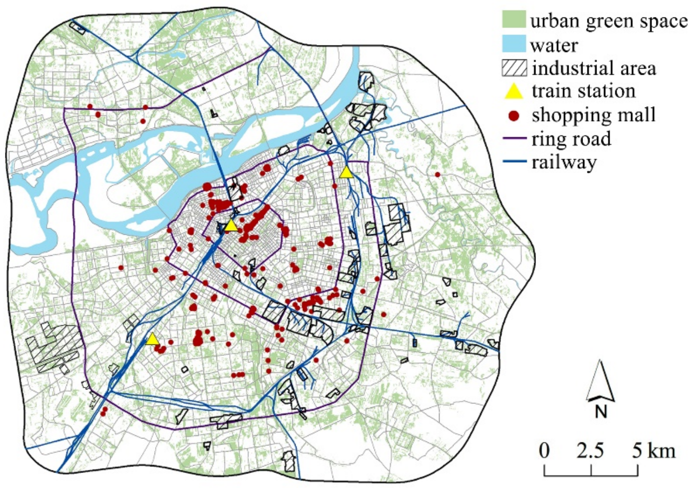

Figure 3. Spatial distribution of urban green space and related land use. Source: By the authors.

3.2. Effect of urban block categories on LST

The average value of LST in each block type shows that the influence of urban block types on LST is also different day and night (Figure 4). During the day, the average LST of high-rise and high-density blocks is the highest, and that of low-rise and low-density blocks is the lowest. Urban blocks with high building density, including HRHD, HRMD, MRHD, MRMD and LRHD, have high LST. This shows that building density is the key factor affecting the intensity of LST during the day. At night, the highest and lowest block types of LST are still HRHD and LRLD respectively. Blocks with the height of middle and high-rise buildings also show relatively high LST at night. This shows that the building height is related to LST at night.

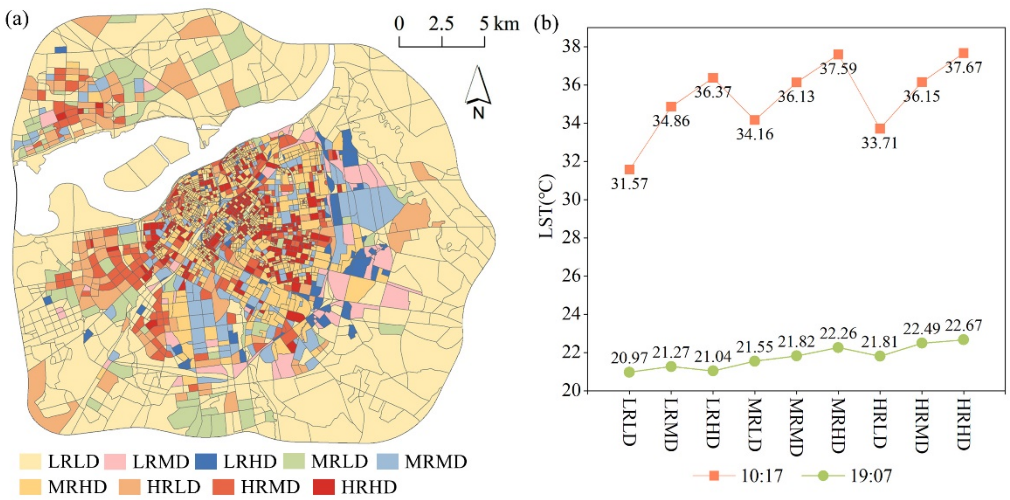

Figure 4. (a) Spatial distribution of urban block categories. The white area in the map has been removed because it was covered by water. (b) Average LST in each urban block category. Source: By the authors.

The calculation results of distribution index (DI) show that HRHD block has the highest distribution index value, which indicates that this kind of block contributes a lot to LST strength (Table 3). The DI values of MRHD and MRMD blocks in both periods exceeded 1. This shows that these two types of blocks are also important heat sources in the study area. In addition, the blocks of HRMD, HRLD, MRLD and LRHD also have a significant impact on the LST intensity at night.

Table 3. The distribution index (DI) of urban block categories at the observation times.

Urban block category	DI value at 10:17	DI value at 19:07
LRLD	0.02	0.08
LRMD	0.04	0.51
LRHD	0.89	1.74
MRLD	0.05	1.29
MRMD	0.99	1.69
MRHD	5.95	2.96
HRLD	0.12	1.41
HRMD	0.62	2.48
HRHD	7.82	5.47

3.3. Influence of urban green space morphological characteristics on LST

Table 4 lists the correlation coefficient between urban green space landscape pattern index and LST. The calculation results show that there is a significant correlation between all indexes and LST. Among them, CA, PLAND, LSI and AI are negatively correlated with LST, while PD is positively correlated with LST. In view of the difference between day and night, LSI and LST in all block categories are negatively correlated during the day. PLAND is negatively correlated with LST in all blocks except LRLD and MRLD. This may indicate that larger area, higher proportion and more dispersed green patches will help to reduce the LST during the day. At night, the relationship between CA, PLAND, LSI and LST is weakened, but it is still significant. This shows that the small cold islands formed by scattered green spaces effectively reduce the LST at night.

Additionally, AI values negatively correlate with LST in LRLD, LRMD, and MRMD blocks during the day, while positively correlating in LRHD blocks at night. This suggests that aggregated green space patches provide cooling during the day but may contribute to warming at night, possibly due to water vapor from vegetation acting as a greenhouse gas, enhancing nighttime thermal insulation. Regarding PD, LRLD, MRLD, and high-rise low-density (HRLD) blocks exhibit significant positive correlations with LST during the day, with LRLD maintaining this correlation at night. This commonality of low building density suggests that increasing the number of green space patches in low-density urban blocks may not effectively enhance cooling.

Table 4. Correlation between LST and urban green space morphological characteristics in different block categories.

Urban block category	CA	PLAND	LSI	AI	PD
10:17-Daytime					
All	-0.495**	-0.366**	-0.512**	-0.223**	0.215**
LRLD	-0.357**	0.047	-0.345**	-0.115**	0.378**
LRMD	-0.494**	-0.456**	-0.423**	-0.356**	0.113
LRHD	-0.423**	-0.318**	-0.231*	-0.133	-0.055
MRLD	-0.427**	0.159	-0.419**	-0.049	0.344**
MRMD	-0.418**	-0.388**	-0.449**	-0.205**	0.095
MRHD	-0.246**	-0.310**	-0.250**	-0.067	-0.122*
HRLD	-0.613**	-0.197*	-0.517**	-0.157	0.303**
HRMD	-0.383**	-0.277**	-0.391**	-0.159*	0.072
HRHD	-0.371**	-0.201**	-0.275*	-0.101	-0.123*
19:07-Nighttime					
All	-0.350**	-0.220**	-0.460**	-0.157**	0.147**
LRLD	-0.226**	-0.115**	-0.357**	-0.066	0.203**
LRMD	-0.139	-0.092	-0.146	0.121	0.027
LRHD	-0.184	0.140	-0.315**	0.295**	0.210
MRLD	-0.410**	0.019	-0.366**	-0.107	0.100
MRMD	-0.370**	-0.239**	-0.367**	-0.099	0.079
MRHD	-0.272**	-0.255**	-0.334**	-0.095*	-0.086*
HRLD	-0.300**	-0.197*	-0.383**	-0.088	0.093
HRMD	-0.063	-0.055	-0.120	-0.046	0.097
HRHD	-0.317**	-0.201**	-0.275**	-0.101	-0.061

Notes : * and ** denote P＜0.05 and P＜0.01 (2-tailed), respectively.

3.4. Main driving factors of LST

All statistically significant urban green space morphological characteristics were entered into stepwise regression models. Separate models were created for all blocks and 9 block categories (Table 5). Considering all blocks, urban green space morphological drivers explained 36.8% of the daytime LST variation and 23.4% of the nighttime LST variation. Specifically, CA was a significant driver of LST during the day for most block categories (except MRMD and HRMD). For LRLD, LRHD, MRHD, HRLD, and HRHD at night, the significant driver became LSI.PLAND and PD were stronger drivers of LST during the day than at night.AI had a weak or irrelevant driving influence on LST in most block categories. Overall, our results suggest to some extent that increasing the area and proportion of green space is an effective measure to reduce LST during the daytime, while increasing the discrete degree of green space patches is an effective way to reduce LST at night.

Table 5. Standardized regression coefficients between urban green space morphological characteristics and LST for different block categories.

Urban block category	CA	PLAND	LSI	AI	PD	R^2
10:17-Daytime						
All	-0.154**	-0.259**	-0.322**	×	0.155**	0.368
LRLD	-0.194**	×	-0.131*	×	0.303**	0.225
LRMD	-0.385**	-0.327**	×	×	×	0.316
LRHD	-0.423**	×	×	×	×	0.168
MRLD	-0.416**	0.244*	×	×	0.228*	0.267
MRMD	×	-0.313**	-0.389**	×	×	0.289
MRHD	-0.157**	-0.255**	×	×	×	0.115
HRLD	-0.445**	×	-0.230**	×	0.147*	0.423
HRMD	×	×	-0.393**	-0.166*	×	0.171
HRHD	-0.317**	×	×	×	×	0.098
19:07-Nighttime						
All	×	-0.135**	-0.416**	×	0.095**	0.234
LRLD	×	×	-0.327**	×	0.124**	0.138
LRMD	×	×	×	×	×	×
LRHD	×	×	-0.274**	0.322**	0.270*	0.208
MRLD	-0.410	×	×	×	×	0.158
MRMD	-0.370**	×	×	×	×	0.133
MRHD	×	-0.130**	-0.274**	×	×	0.122
HRLD	×	×	-0.383**	×	×	0.140
HRMD	×	×	×	×	×	×
HRHD	×	×	-0.168**	×	×	0.025

Notes :* and ** denote P＜0.05 and P＜0.01, respectively. × indicates that the metrics were not considered in the final model.

4. Discussion

4.1. Implications for urban planning

The results of this study suggest that focusing on the daytime thermal environment alone is not sufficient to develop strategies to mitigate the effects of SUHI, and that the nighttime thermal environment should also be considered. The effects of urban green space form indicators on surface temperature (LST) in different block types differed between day and night. Specifically (1) the spatial distribution of LST varies significantly between day and night. Higher daytime LST indicates that urban landscapes (e.g., buildings, water bodies, and woodlands) strongly influence the spatial pattern of LST under strong solar radiation; regions of high intensity of nighttime LST are characterized by water bodies and areas of medium- to high-rise buildings. (2) The effect of urban block class on LST varies with diurnal and nocturnal heat differences. During daytime, building density dominates the magnitude of LST intensity, while at night it may be related to building height. The DI differences in urban block categories during day and night show that high-rise, high-density blocks contribute significantly to LST intensity during both day and night. (3) The results of correlation analysis and stepwise regression modeling suggest that increasing the area and proportion of green space is an effective measure to reduce LST during the daytime, while increasing the discrete degree of green space patches is an effective way to reduce LST at night.

4.2. Limitations and prospects

This study highlights the value of ECOSTRESS-derived LST data for understanding diurnal thermal differences in urban blocks, providing new insights into thermal environment mitigation in high-density areas. However, due to the lack of long time series of continuous LST observations, ECOSTRESS LST using only 2 observation times, especially the LST data excluding the hottest moments, may not be able to fully characterize the diurnal variation of LST. The availability of longer ECOSTRESS records in the future will help to more accurately reveal the diurnal variability of LST at finer scales. Second, although this study identified different effects of urban block type and green space morphological features on daytime and nighttime LST, it did not propose a joint strategy to mitigate the effects on both LSTs simultaneously. In future studies, it would be beneficial to determine the optimal range of daytime and nighttime LST reductions by incorporating a more comprehensive set of urban form factors and considering the variation in the marginal effects of urban form characteristics on daytime and nighttime LST. Third, although the stepwise regression analysis carried out effectively identified the main drivers, it is essentially a linear regression-based approach that may not reveal the nonlinear relationship between the explanatory variables and LST. Therefore, in the future, machine learning-based nonlinear models can be used to jointly explore the quantitative relationship between urban characteristics and LST.

5. References

Chang, Y. *et al.* (2021) 'Exploring diurnal thermal variations in urban local climate zones with ECOSTRESS land surface temperature data', *Remote Sensing of Environment*, 263, p. 112544. Available at: https://doi.org/10.1016/J.RSE.2021.112544.

Chen, K. *et al.* (2023) 'Evaluating the seasonal effects of building form and street view indicators on street-level land surface temperature using random forest regression', *Building and Environment*, 245, p. 110884. Available at: https://doi.org/10.1016/J.BUILDENV.2023.110884.

Hook, S.J. *et al.* (2020) 'In-Flight Validation of the ECOSTRESS, Landsats 7 and 8 Thermal Infrared Spectral Channels Using the Lake Tahoe CA/NV and Salton Sea CA Automated Validation Sites', *IEEE Transactions on Geoscience and Remote Sensing*, 58(2), pp. 1294–1302. Available at: https://doi.org/10.1109/TGRS.2019.2945701.

Hu, D. *et al.* (2022) 'How do urban morphological blocks shape spatial patterns of land surface temperature over different seasons? A multifactorial driving analysis of Beijing, China', *International Journal of Applied Earth Observation and Geoinformation*, 106, p. 102648. Available at: https://doi.org/10.1016/J.JAG.2021.102648.

Huang, X. and Wang, Y. (2019) 'Investigating the effects of 3D urban morphology on the surface urban heat island effect in urban functional zones by using high-resolution remote sensing data: A case study of Wuhan, Central China', *ISPRS Journal of Photogrammetry and Remote Sensing*, 152, pp. 119–131. Available at: https://doi.org/10.1016/J.ISPRSJPRS.2019.04.010.

Hulley, G. *et al.* (2019) 'New ECOSTRESS and MODIS Land Surface Temperature Data Reveal Fine-Scale Heat Vulnerability in Cities: A Case Study for Los Angeles County, California', *Remote Sensing*, 11(18), p. 2136. Available at: https://doi.org/10.3390/RS11182136.

Peng, J. *et al.* (2024), 'Response of urban green space cooling effect to urbanization in the Three Ring Road area of Changsha City', *Sustainable Cities and Society*, 109, p. 105534. Available at: https://doi.org/10.1016/J.SCS.2024.105534.

Peng, J. *et al.* (2018) 'Spatial-temporal change of land surface temperature across 285 cities in China: An urban-rural contrast perspective', *Science of The Total Environment*, 635, pp. 487–497. Available at: https://doi.org/10.1016/J.SCITOTENV.2018.04.105.

Santamouris, M. (2020) 'Recent progress on urban overheating and heat island research. Integrated assessment of the energy, environmental, vulnerability and health impact. Synergies with the global climate change', *Energy and Buildings*, 207, p. 109482. Available at: https://doi.org/10.1016/J.ENBUILD.2019.109482.

Shi, Q. *et al.* (2023) 'UGS-1m: fine-grained urban green space mapping of 31 major cities in China based on the deep learning framework', *Earth System Science Data*, 15(2), pp. 555–577. Available at: https://doi.org/10.5194/ESSD-15-555-2023.

Silvestri, M. *et al.* (2020) 'First Comparisons of Surface Temperature Estimations between ECOSTRESS, ASTER and Landsat 8 over Italian Volcanic and Geothermal Areas', *Remote Sensing*, 12(1), p. 184. Available at: https://doi.org/10.3390/RS12010184.

Stewart, I.D. and Oke, T.R. (2012) 'Local Climate Zones for Urban Temperature Studies', *Bulletin of the American Meteorological Society*, 93(12), pp. 1879–1900. Available at: https://doi.org/10.1175/BAMS-D-11-00019.1.

Sun, F. *et al.* (2020) 'The effects of 3D architectural patterns on the urban surface temperature at a neighborhood scale: Relative contributions and marginal effects', *Journal of Cleaner Production*, 258, p. 120706. Available at: https://doi.org/10.1016/J.JCLEPRO.2020.120706.

Welegedara, N.P.Y., Agrawal, S.K. and Lotfi, G. (2023) 'Exploring spatiotemporal changes of the urban heat Island effect in high-latitude cities at a neighbourhood level: A case of Edmonton, Canada', *Sustainable Cities and Society*, 90, p. 104403. Available at: https://doi.org/10.1016/J.SCS.2023.104403.

Yao, X. *et al.* (2023) 'Exploring the diurnal variations of the driving factors affecting block-based LST in a "Furnace city" using ECOSTRESS thermal imaging', *Sustainable Cities and Society*, 98, p. 104841. Available at: https://doi.org/10.1016/J.SCS.2023.104841.

Yao, X. *et al.* (2022) 'Investigating the effects of urban morphological factors on seasonal land surface temperature in a "Furnace city" from a block perspective', *Sustainable Cities and Society*, 86, p. 104165. Available at: https://doi.org/10.1016/J.SCS.2022.104165.

Zhao, H., Fang, Y. and Xu, X. (2024) 'Quantifying morphology evolutions of urban heat islands and assessing their heat exposure in a metropolis', *Sustainable Cities and Society*, 102, p. 105244. Available at: https://doi.org/10.1016/J.SCS.2024.105244.

Zhou, Y. *et al.* (2022) 'Exploring surface urban heat island (SUHI) intensity and its implications based on urban 3D neighborhood metrics: An investigation of 57 Chinese cities', *Science of The Total Environment*, 847, p. 157662. Available at: https://doi.org/10.1016/J.SCITOTENV.2022.157662.